Indian Journal of Pure & Applied Physics
Vol. 59, June 2021, pp. 437-446

Spectroscopic, Structural, Aromaticity and Electronic Properties of Isatoic Anhydride - Experimental and Theoretical Investigations

Akın Azizoglu[a*] & Cem Burak Yildiz[b]

[a]Department of Chemistry, Faculty of Arts & Sciences, University of Balikesir, TR-10145 Balikesir, Turkey

[b]Department of Aromatic Plants, Vocational School, University of Aksaray, TR-68100 Aksaray, Turkey

Received 15 February 2021; accepted 20 April 2021

The paper compares the experimental FT-IR, ^{1}H- and ^{13}C-NMR spectra of isatoic anhydride (ISA) with the Hartree-Fock (HF) and Density Functional Theory (DFT) calculations using three different basis sets (6-31+G(d,p), 6-311+G(d,p), cc-pVTZ). The best compatibility between the experimental and theoretical FT-IR spectrum was observed with the use of B3LYP/6-31+G(d,p) method for ISA. Furthermore, the theoretical^{1}H- and ^{13}C-NMR spectra interpreted by GIAO method depict that the DFT formalism, particularly the B3LYP/6-311+G(d,p) theory of level, gives an accurate description of the ISA experimental chemical shifts. The calculated structural data were also compared with experimental findings. The statistical regression analyses show that the B3LYP/6-31+G(d,p) method results in a correct description of the ISA crystallographic data. Moreover, the frontier molecular orbitals (FMOs), molecular electrostatic potential (MEP) map, and NBO atomic charges of the ISA have been discussed at B3LYP/6-31+G(d,p) theory of level. The FMO analysis were used to determine the charge transfer within ISA and some chemical descriptors such as ionization potential, electron affinity, chemical hardness, softness, chemical potential and electro negativity. The Nucleus-Independent Chemical Shifts (NICS) were also computed for ISA derivatives, **2-10**. In the X: O and Y: S derivative, **4**, sulphur substitution increases slightly the aromaticity of ISA skeleton.

Keywords: NMR, FTIR, HOMO, LUMO, NICS[1]

1 Introduction

Isatoic anhydride (2H-3,1-Benzoxazine-2,4(1H)-di one, ISA), also known as isatoic acid an hydride, is the condensation product from a*nthranilicacid* (o-amino-benzoicacid) and phosgene or ethyl chloroformate as the source of carbonyl group. A lot of scientific reports describing the synthetic potencies of the ISA reaction have been published[1]. It is very versatile starting organic compound for the synthesis of various heterocyclics[1,2]. Recently, this compound has been also found application as an agent for clinical diagnosis in biological research[3] and as starting material for the synthesis of various antimicrobial agents[4]. Due to the ease of its reactions with electrophiles or nucleophiles, its analogs and derivatives have been used in the manufacture of various agrochemicals, and diverse industrial chemicals[5-8]. Unlike its experimental counterpart, it has been little examined using theoretical models. We found few reports in literature: one for studying the aromatic character of ISA with the isodesmic reaction, a combined experimental and theoretical investigation at the B3LYP/6-311G (d,p) method, and it was deduced that it has some aromatic stabilization[9]. Another one was for investigating the isomerization energy of ISA, at both B3LYP/6-31G(d) and B3LYP/6-311G(d) levels[10]. Recently, Ramos-Morales and et al. reported the local reactivity of ISA to show the best sites for a nucleophilic attack and for an electrophilic attack using local reactivity indices such as: local softness, condensed Fukui function, relative electrophilicity index, and relative nucleophilicity index at the B3LYP/cc- pVTZ method[11]. The literature survey reveals that to the best of our knowledge there was no detailed study on spectroscopic and electronic properties of ISA. This motivates to do the structural analysis, spectroscopic analysis, electronic properties, and aromaticity of the molecules with density functional theory (DFT) and *ab-initio* Hartree Fock (HF) calculations. In this attempt, a complete vibrational spectroscopic investigation has been performed on the molecules to present a detailed assignment of bands in FT-IR spectra on the basis of normal coordinate analysis (NCA)[12-14]. Hence, we wish to report the optimized geometry and the detailed spectroscopic analyses (FT-IR and NMR) of the ISA with the help of

*Corresponding Author
(E-mail: azizoglu@balikesir.edu.tr)

theoretical and experimental methods. The HOMO and LUMO analyses have been also used to elucidate information regarding charge transfer within the ISA.

2 Experimental Analyses

2.1 Chemicals and instrumentation

All chemicals and reagents used were purchased from Sigma-Aldrich Company, and hence the sample was used without further purification. The FT-IR spectrum of ISA was recorded by KBr pellet technique in Perkin-Elmer 180 Spectrometer between 4000 cm^{-1} and 400 cm^{-1}.In this experiment sample is prepared by KBr pellet method and spectrum is recorded using DTGS detector at spectral resolution 2 cm^{-1}. The ^{1}H-NMR and ^{13}C-NMR spectra has been also recorded in the Bruker Avance 400 MHz spectrometer. The NMR spectra were obtained in DMSO solvent. Chemical shifts were reported in ppm relative to tetra methylsilane (TMS).

2.2 Synthesis

The green reaction of isatin (**1**) with acetic anhydride and acetic acid in presence of urea-hydrogen peroxide complex under ultrasonic irradiation yielded isatoic anhydride (3,1-Benzoxazine-2,4(1H)-dione, **2**)as depicted in Scheme 1[15]. The product was crystallized from acetic acid. The obtained crystals were used to examine the spectroscopic properties of ISA.

3 Computational Details

The geometry of ISA was fully optimized without any constraints from X-ray diffraction data[16].The most stable conformation of ISA on the potential energy surface (PES) was computed by using the exchange-correlation functional B3LYP[17], the hybrid functional of Truhlar and Zhao M06[18], and the ab-initio HF methods[19]in combination with the Pople basis sets, 6-31+G(d,p) , 6-311+G(d,p)[20], and the correlated Dunning basis set, cc-pVTZ[21]. The calculations have been performed with Gaussian 09 software package[22]. The vibration frequencies of the ISA were calculated at the corresponding levels. The ^{1}H-NMR and ^{13}C-NMR chemical shifts were studied using Gauge Including Atomic Orbital (GIAO) method to compare experimental findings, one of the most common approaches for calculating nuclear magnetic shielding tensors[23,24]. In order to determine reactive sides of the title molecule, we have performed molecular electrostatic potential (MEP) calculations. MEP, V(***r***), is described with regard to the interaction energy between the electrical charge (electrons and nuclei) and positive charge (protons) of molecule located at ***r***. The V(***r***) value for the studied system was gained from the following Eq. 1[25].

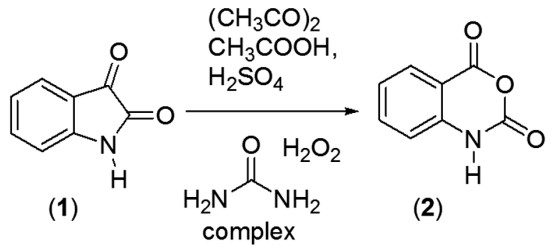

Scheme 1 —General scheme for the synthesis of ISA (3,1-Benzoxazine-2,4(1H)-dione, **2**)

$$V(r)\sum\frac{Z_A}{|R_A-r|}-\int\frac{p(r')}{|r'-r|}dr' \quad \ldots(1)$$

Where Z_A means the charge of nucleus *A*. The $\rho(r')$ is the electronic density function of the molecule and *r'* is the dummy integration variable.

The frontier molecular orbitals (HOMO-LUMO) have been calculated to determine the molecular chemical stability of the structure at B3LYP/6-31+G(d,p) theory of level. The ionization potential (*I*), electron affinity (A), chemical hardness (η), softness (s),chemical potential (μ) and electronegativity (χ) calculations were also obtained from computed HOMO-LUMO energy values in accordance with following equations (2-7)[26,27].

$$I = -E_{HOMO} \quad \ldots(2)$$

$$A = -E_{LUMO} \quad \ldots(3)$$

$$\eta = \frac{E_{LUMO}-E_{HOMO}}{2} \quad \ldots(4)$$

$$s = 1/2\,\eta \quad \ldots(5)$$

$$\mu = \frac{E_{HOMO}+E_{LUMO}}{2} \quad \ldots(6)$$

$$\chi = -\mu \quad \ldots(7)$$

Finally, the Nucleus-Independent Chemical Shifts (NICS), NBO charges, and Mulliken charges were also calculated at B3LYP/6-31+G(d,p) theory of level. The visualizations were animated with the help of the Gauss View 03 program[28].

4 Results and Discussion

4.1 Molecular Geometry

To clarity the vibrational frequencies and NMR chemical shifts, it is essential to understand the

geometry of any compound as structure determines properties. The optimized geometry of Isatoic Anhydride (**2**, ISA) with atoms numbering are shown in Fig. 1. The bond lengths and bond angles of ISA are calculated at HF, B3LYP, and M06 methods in combination with 6-31+g(d,p), 6-311+G(d,p), cc-p VTZ basis sets. In order to compare the experimental and theoretical bond lengths and bond angles for ISA, correlation graphic values based on the calculations have been also computed by regression coefficient analysis. The R^2 value is calculated to be 0,967, 0,966, 0,969, 0,936, 0,931, 0,930, 0,944, 0,937, and 0,938, respectively for HF/6-31+G(d,p), HF/6-311+G(d,p), HF/cc-pVTZ, B3LYP/6-31+G(d,p), B3LYP/6-311+G(d,p), B3LYP/cc-pVTZ, M06/6-31+G(d,p), M06/6-311+G(d,p), and M06/cc-pVTZ levels. This confirms that computed geometry at HF/cc-pVTZ shows excellent matching with the experimental data. For instance, the calculated bond lengths of N1-C2, O3-C4, C4-C5, and C7-C8 determined to be 1,359 Å, 1,361Å, 1,467 Å, 1,391 Å and that of experimental values are 1,342 Å, 1,339 Å, 1,454 Å, 1,379 Å, respectively[16]. Especially, the calculated value C6-C7 (1.391 Å) distance is found to be very similar to the experimental value of 1.389 Å for ISA at the HF/cc-pVTZ method, which is again longer than the experimental values of similar structure. The calculated C-H bond lengths in the phenyl ring are almost equal to 1.0 Å, which are in agreement with standard data. Hence, the values of bond lengths in the phenyl and hetero ring are in fair agreement with those from the theoretical calculations. However, the N1-C2 is somewhat shorter and C2-O11 is longer than the computed values The planarity of hetero ring indicates that the O and N atoms in the ring have sp^2 hybridization. Moreover, the $R^2$for bond angles are found to be 0,852,0,848,0,858,0,889,0,877,0,880,0,857,0,852, and 0,858 at HF/6-31+G(d,p), HF/6-311+G(d,p), HF/cc-pVTZ, B3LYP/6-31+G(d,p), B3LYP/6-311+G(d,p), B3LYP/cc-pVTZ,M06/6-31+G(d,p), M06/6-311+G (d,p), and M06/cc-pVTZ, respectively, thus it can be deduced that the bond angles of ISA predicted at B3LYP/6-31+G(d,p) are closer to the experimental values. The most compatible structural data are also summarized in Table 1. The C-N-C angle at B3LYP/6-31+G(d,p) is found to be 124,1°, which is

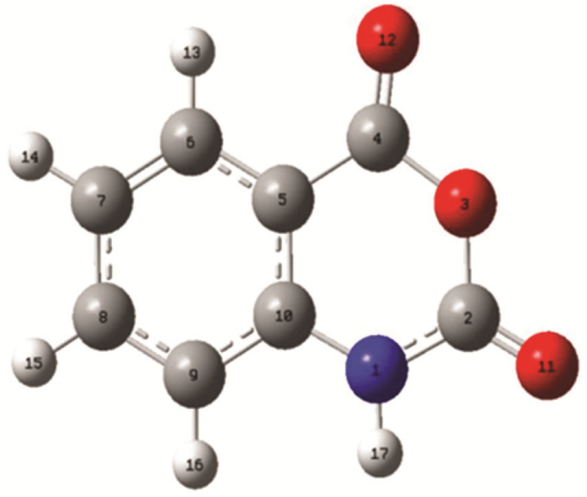

Fig. 1 — Optimized geometric structure of ISA along with atoms numbering.

Table 1 — Optimized geometrical parameters of ISA at HF/cc-pVTZ and B3LYP/6-31+G(d,p) levels in comparison with experimental data[16]

Bond Lengths (Å)	Exp.[a]	HF/ cc-pVTZ	B3LYP/ 6-31+G(d,p)
N1-C2	1,342	1,359	1,378
C2-O11	1,213	1,176	1,207
C2-O3	1,352	1,339	1,374
O3-C4	1,339	1,361	1,402
C4-O12	1,189	1,172	1,204
C4-C5	1,454	1,467	1,468
C5-C10	1,376	1,381	1,404
C10-N1	1,393	1,38	1,390
C10-C9	1,392	1,388	1,402
C9-C8	1,389	1,375	1,392
C8-C7	1,379	1,391	1,404
C7-C6	1,389	1,391	1,390
C6-C5	1,406	1,389	1,403
R^2	-	0,969	0,936
N1-C2-O11	125,1	123,5	123,8
N1-C2-O3	116,5	115,8	115,5
N1-C10-C5	119,5	118,4	118,4
C10-C5-C4	118,5	118,9	119,4
C5-C4-O3	116,1	115,7	115,9
C5-C4-O12	127,9	126,0	126,5
O12-C4-O3	115,9	118,3	117,6
O3-C2-O11	118,4	120,7	120,7
C10-N1-C2	124,1	124,5	125,1
C2-O3-C4	125,1	126,7	125,7
C6-C5-C10	120,2	120,3	120,0
C7-C6-C5	119,2	120,1	120,1
C8-C7-C6	119,9	119,2	119,6
C9-C8-C7	121,2	121,4	121,1
C10-C9-C8	118,9	119,0	119,3
C9-C10-C5	120,6	120,1	120,1
N1-C10-C9	119,9	121,5	121,5
C4-C5-C6	121,3	120,9	120,6
R^2	-	0,858	0,889

significantly larger than the classical sp^2 angle. From this fact and the length of the exocyclic C2-O11bond, it can be concluded that the ketonic form is the preferred tautomer in the solid state. Small differences in the angles of ISA between theoretical and experimental values are observed about the studied bonds. These minor discrepancies are incorporated because of our isolated model selected for theoretical calculations, while experimental values involve intermolecular interactions originated by solid state of the crystal.

4.2 Vibrational spectra

Molecular vibrations are most useful tools in from both experimental and computational communities. Modern vibrational spectrometry is an effective method to solve many chemical problems. Vibrational spectroscopy has also been shown to be effective in the description of functional groups of organic compounds[29]. The detailed spectroscopic signature of ISA has not yet been studied to the best of our knowledge. The compound of ISA consists of 17 atoms, and it has 45 normal modes of vibrations under C1 point group symmetry and all vibrations are active in infrared absorption. The vibrational spectral assignments have been carried out on the recorded FT-IR spectra based on theoretically predicted wave numbers by HF, B3LYP, and M06 methods with 6-31+G(d,p), 6-311+G(d,p), cc-pVTZ basis sets. The stretching (ν), symmetrical stretching (ν_s), asymmetrical stretching (ν_{as}), scissoring (δ), rocking (ρ),twisting (t), wagging (ω) modes of the ISA are described in their characteristic regions and contribute to several normal modes. In order to expedite assignment of the predicted peaks, we have analyzed the vibrational frequencies and compared our theoretical calculations with the experimental results (Table 2).

It is well known that experimental results of infrared spectroscopy usually lower than the corresponding computational quantities, due to the combination of electron correlation effects and basis set deficiencies. The experimental and theoretical FT-IR spectra of the title compound are shown in Fig. 2. On comparing the theoretical values with experimental values, they show pronounced shifts in the spectra due to hydrogen bonding interactions especially in NH, O-C=O, C=O group vibrations due to HN···O-C=O, C=O···NH interactions and electron correlation effects, which can distort symmetry and also normal values. FT-IR spectra of the title structure are dominated by a broad and intense absorption in the range 600-2200 cm^{-1} with O=C and C-N vibrations. We have also correlated the experimental and theoretical FT-IR results and obtained R^2 values which are calculated to be 0.9958 for HF/6-

Table 2 — Calculated and observed normal mode frequencies

No	Exp.	B3LYP/6-31+G(d,p)	Assignment*
1		3635	$\nu(N^1\text{-}H^{17})$
2		3226	$\nu_s(CH_{ring})$
3	3240	3214	$\nu_{as}(CH_{ring})$
4	3172	3202	$\nu_{as}(CH_{ring})$
5	3105	3189	$\nu_{as}(CH_{ring})$
6	1763	1860	$\nu_s(C^4{=}O^{12})$: $\nu_s(C^2{=}O^{11})$
7	1723	1816	$\nu_{as}(C^4{=}O^{12})$: $\nu_{as}(C^2{=}O^{11})$
8		1662	$\nu(C_{ring}{=}C_{ring})$
9	1615	1641	$\nu(C_{ring}{=}C_{ring})$
10	1599	1531	$\nu(C_{ring}{=}C_{ring})$: $\delta(CH_{ring})$
11	1513	1528	$\nu(C_{ring}{=}C_{ring})$: $\delta(CH_{ring})$
12	1439	1449	$\delta(N^1\text{-}H^{17})$: $\rho(CH_{ring})$
13	1362	1377	$\nu(C_{ring}{=}C_{ring})$
14	1330	1349	$\nu(C^2\text{-}N^1)$: $\rho(CH_{ring})$
15	1296	1289	$\nu(N^1\text{-}C^{10})$: $\delta(CH_{ring})$
16	1261	1263	$\rho(N^1\text{-}H^{17})$: $\rho(CH_{ring})$
17	1214	1215	$\nu(C^2\text{-}N^1)$: $\delta(CH_{ring})$
18		1182	$\delta(CH_{ring})$
19	1123	1138	$\delta(CH_{ring})$
20	1105	1063	$\delta(CH_{ring})$
21	1038	1027	$\nu(C^2\text{-}O^3\text{-}C^4)$
22	1007	1004	$t(CH_{ring})$
23	987	983	$\nu(C^2\text{-}N^1)$
24	967	980	$t(CH_{ring})$
25	907	909	$\delta(N^1\text{-}H^{17})$: $\delta(CH_{ring})$
26	877	875	t(CHring)
27	787	785	$\omega(CH_{ring})$
28		765	$\rho(CH_{ring})$
29		762	$t(CH_{ring})$
30	746	731	$t(C^2\text{-}N^1)$
31		689	$\delta(C^4\text{-}O^{12})$: $\delta(CH_{ring})$
32	680	688	$t(C^2\text{-}O^{11})$: $t(CH_{ring})$
33	648	642	$\rho(C^9\text{-}H^{16})$: $\rho(N^1\text{-}H^{17})$, $\delta(C^2\text{-}O^{11})$
34		561	$t(N^1\text{-}H^{17})$
35		561	$\nu(C^4\text{-}O^{12})$: $\nu(CH_{ring})$, $\nu(N^1\text{-}H^{17})$
36		526	$t(CH_{ring})$: $t(N^1\text{-}H^{17})$
37		468	$\delta(C^2\text{-}O^3\text{-}C^4)$: $\delta(C^8\text{-}H^{15})$
38		455	$\nu(C^2{=}O^{11})$: $\nu(C^7\text{-}H^{14})$
39		427	$t(CH_{ring})$
40		381	$\delta(O^{11}\text{-}C^2\text{-}O^3\text{-}C^4\text{-}O^{12})$
41		281	$\rho(C^9\text{-}H^{16})$: $\delta(C^4\text{-}O^{12})$
42		258	$t(CH_{ring})$: $t(N^1\text{-}H^{17})$
43		150	$t(CH_{ring})$: $t(N^1\text{-}H^{17})$
44		133	$t(C^2\text{-}O^3\text{-}C^4)$: $t(N^1\text{-}H^{17})$
45		76	$t(C^2\text{-}N^1)$

*ν: stretching, νs: symmetrical stretching, νas: asymmetrical s scissoring, ρ: rocking, t: twisting, ω: wagging

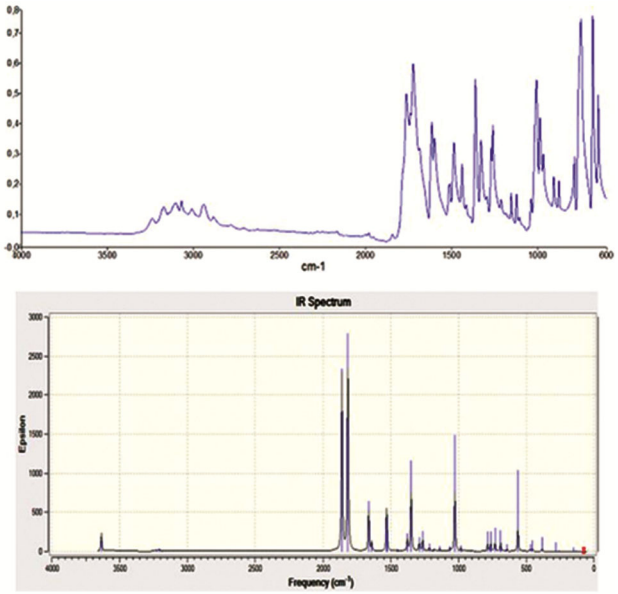

Fig. 2 — Theoretical (B3LYP/6-31+G(d,p)) and experimental FT-IR spectra of ISA.

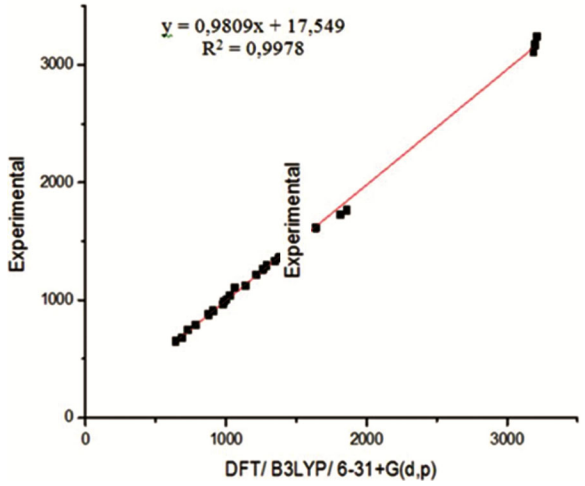

Fig. 3 — The correlation between the experimental and theoretical wavenumbers.

31+G(d,p), 0.9957 for HF/6-311+G(d,p), 0.9956 for HF/cc-pVTZ, 0.9978 for B3LYP/6-31+G(d,p), 0.9976 for B3LYP/6-311+G(d,p), 0.9977 for B3LYP/cc-pVTZ, 0.9961 for M06/6-31+G(d,p), 0.9959 for M06/6-311+G(d,p), 0.9960 for M06/cc-pVTZ level. Hence, experimental findings have slightly a better correlation for B3LYP/6-31+G(d,p) than others (Fig. 3). As seen from calculated R^2values, the agreements between the experimental and theoretical results are acceptable and not need any scaling factor to apply.

The C-H stretching vibrations are expected to appear in the region of 3250 cm^{-1} -3100 cm^{-1} with multiple strong bands. The calculated vibrational wave numbers of the title compound are observed at 3189 cm^{-1}, 3202 cm^{-1}, 3214 cm^{-1}, 3226 cm^{-1} for C-H stretching at B3LYP/6-31+G(d,p) theory of level. The experimental in-plane C-H bending vibrations were observed strong band at 1007 cm^{-1}. The calculated band at B3LYP/6-31+G(d,p) level is determined at 1004 cm^{-1}, well correlated with the FT-IR spectrum.

The C-N stretching mode is normally assigned between 1080-1360 cm^{-1} for chemical systems. The molecule has two C-N stretching vibrations. The C10-N stretching vibration is appeared at 1330 cm^{-1}. The calculated C10-N stretching band was calculated to be 1349 cm^{-1} at B3LYP/ 6-31+G(d,p) theory of level. On the other hand, the C2-N stretching band was observed at 987 cm^{-1} with weak band. The calculated C2-N stretching band which is obtained from B3LYP/6-31+G(d,p) theory of level was calculated at 983 cm^{-1}.

The C=O vibrations are marginally to be the most sensitive for the structures. The experimental C=O stretching vibrations lie in the region between 1723 and 1763 cm^{-1}. The calculated C=O stretching bands observed at 1816 cm^{-1}, 1860 cm^{-1}.The calculated C=O scissoring (bending) band calculated to be 281 cm^{-1} at B3LYP/6-31+G(d,p) theory of level.

The ring stretching vibrations are very important due to characteristic nature in the IR spectrum for the systems which have aromatic ring. The C=C stretching vibrations of the ring appear in the range of 1625–1400 cm^{-1}. In the present molecule, the experimental C=C stretching vibrations of ISA are observed at 1615, 1599, 1362 and 1214 cm^{-1} in the FT-IR spectrum. The calculated C=C stretching bands at B3LYP/6-31+G(d,p) level are in the range from 1215 cm^{-1} to 1641 cm^{-1}.

4.3 NMR spectra

Nuclear Magnetic Resonance (NMR) has long been used to investigate properties of molecules. We can obtain particular information about structural and electronic features of compounds by using NMR technique. ^{1}H and ^{13}C chemical shifts of ISA (with respect to TMS) was studied experimentally and theoretically at the B3LYP/6-31+G(d,p), B3LYP/6-311+G(d,p), and B3LYP/cc-pVTZ theory of levels. To determine the influence of solvent on the structure of the molecule, we first optimized the ISA in dimethyl sulfoxide (DMSO) with the help of IEFPCM method[30]. Then, we have performed ^{1}H-NMR and

^{13}C-NMR calculations by using the GIAO (gauge-including atomic orbital) method[23,24]. The chemical shifts for ^{1}H and ^{13}C are reported in ppm (Table 3). The atom statues were numbered according to Fig. 1. The calculated ^{1}H values of the ring protons are determined to be in the range of 6.85 to 8.60 ppm at B3LYP methods, whereas experimentally observed ^{1}H values are between 7.16 and 7.92 ppm. As for ^{13}C-NMR chemical shift values, the highest ^{13}C value calculated to be 169.1 ppm for C4 atom at B3LYP/6-311+G(d,p) theory of level. On the other hand, the lowest ^{13}C value is 106.0 ppm for C5 atom at B3LYP/6-311+G(d,p) theory of level. On an absolute scale, the calculated ^{1}H and ^{13}C chemical shifts for the title system are in good agreement with experimentally predicted chemical shifts obtained in DMSO are shown in Fig. 4.

4.4 Nucleus Independent Chemical Shifts (NICS)

Aromaticity is considered a cornerstone to predict character of a molecule in modern organic chemistry[31].

Table 3 — Experimental and calculated ^{1}H-NMR and ^{13}C-NMR chemical shifts of ISA

		B3LYP		
	Exp.	6-31+G(d,p)	6-311+G(d,p)	cc-pVTZ
H17	11,70	7,42	7,35	6,66
H13	7,92	8,28	8,35	8,65
H15	7,74	8,05	8,11	7,92
H14	7,26	7,51	7,57	7,32
H16	7,16	7,29	7,35	6,91
C4	159,8	158,7	169,1	164,4
C2	147,0	145,1	155,0	150,5
C10	141,3	138,5	149,5	147,3
C8	136,8	135,4	146,6	141,4
C6	128,8	128,7	138,4	137,5
C7	123,4	121,9	131,7	127,1
C9	115,2	113,3	121,9	116,1
C5	110,0	109,8	115,7	115,2

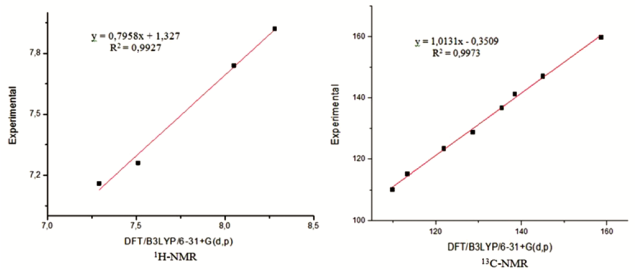

Fig. 4 — The correlations of the experimental and calculated (B3LYP/6-31+G(d,p)) ^{1}H-NMR (Left) and ^{13}C-NMR (Right) chemical shifts for ISA.

Basically aromatic criterion of a molecule depends on number of π-electrons of cyclic-conjugated π-systems. In 1996, Schleyer proposed an effective method to compute aromaticity of a molecule with the value of the negative magnetic shielding at the selected points in ring or cage. This method called as Nucleus Independent Chemical Shift (NICS)[32]. The diamagnetic and paramagnetic effects of ring currents related to aromaticity and antiaromaticity can be also evaluated by NICS criterion[33].In this method, it can be said that a molecule with high negative NICS value is an aromatic compound, whereas high positive NICS value depict that a molecule has an antiaromatic character. On the other hand, low NICS values describe non aromaticity for a molecule. Due to the neglect of the σ contributions, NICS at the 1Å above the center of ring, NICS(1), was recommended to be better aromaticity diagnostic than the NICS(0)[32-35]. Hence, NICS(1) was computed at the B3LYP/6-31+G(d,p) theory of level for ISA and some combinations of X:-O, -S, -CH_2 and Y:-O, -S, -CH_2 in Fig. 5. We desired to determine heteroatom effect on the aromaticity of ISA. The NICS values calculated for the ring 1 and ring 2 separately (Table 4). The findings reveal that the ring 1 has higher aromatic character than ring 2 because of the more negative NICS values indicating the more aromatic the systems. According to NICS calculations, there are small changes in aromaticity as a function of the substitutent heteroatom or the number of replaced X and Y groups, for instance, NICS(1) varies from -7.962 to -9.232 on ring 1. In the X: O and Y: S derivative, **5**, sulphur substitution rises the aromaticity of ISA skeleton. By replacing two oxygens with

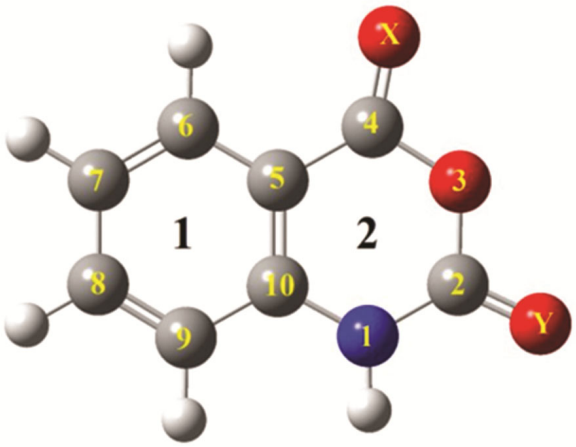

Fig. 5 — ISA, **2**, and its homologues**3**-**10**(X= S, O, or CH_2 and Y= S, O, or CH_2) for NICS(1) calculations.

Table 4 — Calculated NICS(1) values for the Ring 1 (*Italic*) and Ring 2 (**Bold**)

No	X-Y	NICS(1)
2	X=O, Y=O	*-9.141* /**-1.063**
3	X=O,Y=CH_2	*-8.011* / **1.096**
4	X=S, Y=CH_2	*-7.589* / **1.868**
5	X=O, Y=S	*-9.232* /**-0.468**
6	X=CH_2, Y=O	*-8.648* / **0.421**
7	X=CH_2, Y=CH_2	*-7.962* / **1.101**
8	X=S, Y=S	*-8.834* / **0.319**
9	X=S, Y=O	*-9.067* /**-0.635**
10	X=CH_2, Y=S	*-8.672* / **1.186**

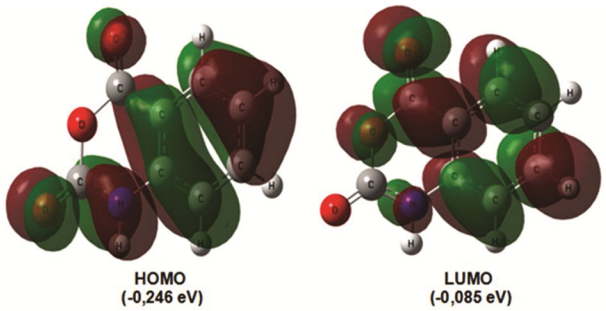

Fig. 6 — The pictorial illustration of FMO of ISA at B3LYP/6-31+G(d,p) theory of level.

sulphur atoms, the NICS values decreased to be -8.834in **8**. The effect of X and Y substitutions in aromaticity is meager. In a previous study by Matos et al., ISA has been identified as a plausible aromatic compound with the calculated energies from its isodesmic reaction[10]. In this case, our further analysis on the aromaticity of ISA denote that total NICS value of ISA prefer an aromatic character. Using data from the NICS analyses of compounds **2**-**10**, it can be concluded that the **4** derivative (X: O and Y: S) is slightly more aromatic than ISA, **2**, but in general, their degree of aromaticity remains moderate.

4.5 Frontier molecular orbitals

The frontier molecular orbitals (highest occupied molecular orbital-HOMO and lowest unoccupied molecular orbital-LUMO) are the main orbitals taking part in chemical reactions[36]. The energies of HOMO and LUMO are calculated using B3LYP/6-31+G(d,p) method and the pictorial illustration of the frontier molecular orbitals are shown in Fig. 6. The DFT-based chemical reactivity description provides valuable information about the reactive sites for various types of attacks and orientation for several compounds[37-40]. In this case, we have applied the same methods for the title system during the studies. The energy of HOMO is often associated with the electron donating ability of the molecule. High E_{HOMO} values define that the molecule has a tendency to donate electrons to appropriate acceptor molecules with low energy empty molecular orbital. The energy of LUMO relates with the ability of the molecule to accept electrons. The lower values of E_{LUMO}, the more probable it is that the molecule can accept electrons.

The HOMO and LUMO analyses were also used to determine the charge transfer within ISA and some chemical reactivity descriptors such as ionization potential (*I*), electron affinity (A), chemical hardness(η), softness (s),chemical potential (μ) and electro negativity (χ). The chemical hardness is an important quantity in chemical reactivity theory and it was first put forward by Pearson[41], which is a measure of the resistance of a chemical species to change its electronic configuration. One should be careful while using orbital energies to calculate chemical hardness, since the orbital energies are strongly dependent on the basis set and exchange correlation potential used in DFT calculations. Hence, the frontier molecular orbital gap ($\Delta E_{LUMO-HOMO}$), ionization potential (*I*), electron affinity (A), chemical hardness(η), softness (s), chemical potential (μ) and electronegativity (χ) chemical descriptors for ISA were calculated at HF and DFT levels studied herein (Table 5). The HOMO–LUMO energy gap is an important kinetic stability index and it also reflects the chemical reactivity of a molecule. A molecule with a small ΔE is more polarizable and is generally associated with a high chemical reactivity, low kinetic stability. One can also relate the stability of a molecule to hardness, which means that the molecule with least ΔE means is more reactive. Soft molecules are large and highly polarizable, while hard ones are relatively small and much less polarizable.

The chemical potential (μ) of the molecule is defined with the help of Koopmans's theorem, which of calculating the potential energy assumes that the electron only interacts with the average charge of the electron cloud[26,27]. As it can be seen in Table 5, the chemical potential is negative remarking that ISA is stable and does not decompose spontaneously into its elements. The hardness points out the resistance towards the deformation of electron cloud of compounds under small perturbations encountered during chemical process.

Table 5 — Calculated molecular properties of ISA from FMO energies (*eV*)

Molecular parameters / Basis set	HF			DFT/B3LYP			M06		
	6-31+G(d,p)	6-311+G(d,p)	cc-pVTZ	6-31+G(d,p)	6-311+G(d,p)	cc-pVTZ	6-31+G(d,p)	6-311+G(d,p)	cc-pVTZ
E_{HOMO}	-0,348	-0,348	-0,345	-0,246	-0,266	-0,261	-0,275	-0,277	-0,270
E_{LUMO}	0,049	0,045	0,062	-0,082	-0,087	-0,080	-0,077	-0,078	-0,069
$\Delta E_{LUMO-HOMO}$	0,397	0,393	0,407	0,164	0,179	0,181	0,198	0,199	0,201
I	0,348	0,348	0,345	0,246	0,266	0,261	0,275	0,277	0,270
A	-0,049	-0,045	-0,062	0,082	0,087	0,080	0,077	0,078	0,069
η	0,198	0,197	0,203	0,082	0,089	0,090	0,099	0,099	0,100
s	2,525	2,538	2,463	6,098	5,618	5,556	5,051	5,051	5,000
μ	-0,149	-0,151	-0,141	-0,164	-0,176	-0,171	-0,176	-0,177	-0,169
χ	0,149	0,151	0,141	0,164	0,176	0,171	0,176	0,177	0,169

4.6 Molecular electrostatic potential

The chemical advantages of ISA as a precursor of a great amount of derivatives lie mainly in its capacity to react through two fundamental mechanisms. One is the reaction of the aromatic ring at C8 toward electrophilic attack, if this position is available, or at C10 if it is occupied by another functional group. The second is the reactivity of the oxirane ring toward nucleophilic attack in the carbon base of the carbonyl group C2, generally losing a CO_2. A third place where a reaction can occur is at the N atom, due to its electronic properties

The molecular electrostatic potential (MEP) maps represent the charge distributions of molecules. These maps afford a pictorial method to define the charged regions as well as the relative polarity of a molecule. Therefore, MEP have been carried out in order to interpret and predict both electrophilic and nucleophilic behaviors in various chemical systems[42-44]. The relative polarity of the molecule can be provided with the help of molecular electrostatic potential (MEP) maps. In the MEPs, the most suitable atomic site for electrophilic attack by protons is described as red color. On the other hand, the positive electrostatic potentials are appeared as blue surface areas where the potentials are closer to zero. The MEP was plotted at the B3LYP/6-31+G(d,p) level for the title compound as shown in Fig. 7. As can be seen from Fig. 7, the oxygen atoms are covered by a greater surface of red color which describes most negative region of the molecule. Maximum positive regions are mainly over the nitrogen atom. Considering this calculated results, the MEP map depicts that behavior of the molecule in the reactions is in accordance with positive and negative sites.

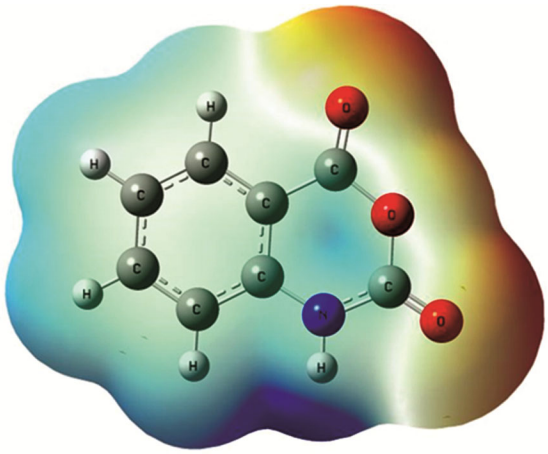

Fig. 7 — 3D-MEP map of ISA calculated at B3LYP/6-31+G(d,p) level.

4.7 NBO charge analysis

The calculation of atomic changes plays an important role in the application of quantum chemistry to molecular systems[45,46]. Natural Bond Orbitals (NBO) atomic charges for the non-H atoms of ISA calculated at B3LYP/6-31+G(d,p), B3LYP/6-311+G(d,p), and B3LYP/cc-pVTZ levels are presented in Table 6. It is worthy to mention that the obtained NBO results do not depend on the level of theory. Generally, the NBO atomic charge values indicate that the carbon atom of carbonyl group (C2) has a bigger positive charge, whereas the nitrogen atom of hetero ring (N1) has a bigger negative charge than others. Moreover, the large negative charges of nitrogen and oxygen atom of hetero ring (N1 and O3) may be related with a nucleophilic suction pump, acting as a possible magnet for electrophilic attack of H+ or part of a biological receptor or probable

Table 6 — NBO charges of ISA

	B3LYP/6-31G(d)	B3LYP/6-31+G(d,p)	B3LYP/6-311+G(d,p)	B3LYP/cc-pVTZ
N1	-0,644	-0,651	-0,617	-0,589
C2	0,947	0,933	0,923	0,883
O3	-0,550	-0,542	-0,549	-0,504
C4	0,811	0,802	0,794	0,773
C5	-0,218	-0,216	-0,212	-0,217
C6	-0,158	-0,164	-0,125	-0,119
C7	-0,256	-0,264	-0,225	-0,224
C8	-0,186	-0,192	-0,148	-0,142
C9	-0,269	-0,275	-0,240	-0,244
C10	0,197	0,194	0,202	0,197
O11	-0,584	-0,588	-0,574	-0,566
O12	-0,539	-0,542	-0,573	-0,525

reactive sites to the metal surface to form a coordinate bond.

5 Conclusions

The experimental and theoretical spectroscopic results (NMR and FT-IR) displayed in the present study. The findings reveal that experimental and theoretical results confirm each other. There is an excellent agreement between experimental results and theoretical calculation for NMR and FT-IR spectroscopy at B3LYP/6-31+G(d,p) theory of level. The calculated geometric parameters show also good agreement with experimentally observed values. The small deviations are observed between experimental and theoretical vibrational modes. This is due to the fact that experimental FT-IR spectra belong to the solid phase and computational ones belong to the gaseous phase. According to the Nucleus Independent Chemical Shift (NICS) criterion, negative NICS values denote aromaticity, positive values anti aromaticity, and values close to zero non aromaticity. It is evident from NICS(1) calculations that the ring 1 has aromatic character, whereas ring 2 has not. The highest negative NICS value determined to be -8.11 (for benzene -9.7) for ring 1 in the structure **1**. The NBO charges and MEP map indicates that the negative potential sites are around the oxygen and nitrogen atoms of ISA while the positive potential sites are around the carbon atoms of carbonyl groups. Besides, the obtained results will help researchers to analysis and synthesis of new ISA derivatives.

Acknowledgements

This research was supported by Balikesir University Scientific Research Projects Unit with the project number *2018/175*. Authors are very grateful to the reviewers' valuable comments that improved our manuscript.

References

1 Kappe T & Stadlbauer W, *Adv Heterocyclic Chem*, 28 (1981) 127.
2 Nawrot B, Milius W, Ejchart A, Limmer S & Sprinz M, *Nucleic Acids Res*, 25 (1997) 948.
3 Weissleder R, Kelly K, Sun EY, Shtatland T & Josephson L, *Nat Biotechnol*, 23 (2005) 1418.
4 Mabkhot Y N, Al-Majid A M, Barakat A, Al-Showiman S S, Al-Har M S, Radi S, Naseer M M & Hadda T B, *Int J Mol Sci*, 15 (2014) 5115.
5 Coppola G M, *Synthes*is, 1980 (1980) 505.
6 Abbas S Y, El-Bayouki K A M & Basyouni W M, *Synth Commun*, 46 (2016) 993.
7 Shvekhgeimer M G A,*Chem Heterocycl Compd*, 37 (2001) 385.
8 Bogdanov A V & Mironov V F,*Chem Heterocycl Compd*, 52 (2016) 90.
9 Matos M A R, Miranda M S, MoraisV M F & Liebman J F, *Org Biomol Chem*, 1 (2003) 2566.
10 Matos M A R, Miranda M S, MoraisV M F & Liebman J F, *Org BiomolChem*, 2 (2004) 1647.
11 Durand-Niconoff J S, Cruz-Kuri L, Cruz-Sánchez J S, Matus M H & Ramos-Morales F R, *Int J Quant Chem*,112 (2012) 3570.
12 Anju L S, Aruldhas D, Hubert Joe I & John N L, *J Mol Struct*,1208 (2020) 12790.
13 Sambathkumar K, *Indian J Pure Appl Phys*, 58 (2020) 589.
14 Yıldız C B, SagirZ O, Kilic T & Azizoglu A, *Studia UBB Chemia*, LIX (2014) 17.
15 Deligeorgiev T, Vasilev A, VaqueroJ J & Alvarez-Builla J, *Ultrason Sonochem*, 14 (2007) 497.
16 Kashino S, Nakashima S & Haisa M, *Acta Cryst*, 34 (1978) 2191.
17 Becke A D, *J Chem Phys*, 107 (1997) 8554.
18 Zhao Y & Truhlar D G, *Theor Chem Acc*, 120 (2008) 215.
19 Roothan C C, *J Rev Mod Phys*, 23 (1951) 69.
20 Hehre W J, Random L, Schleyer P R & Pople J A, Ab Initio Molecular Orbital Theory (Wiley, New York), 1986.
21 Dunning H T, *J Chem Phys*, 90 (1989) 1007.
22 Frisch M J, Trucks G W, Schlegel H B, Scuseria G E, Robb M A, Cheeseman J R, Scalmani G, Barone V, Mennucci B, Peterson G A, Nakatsuji H, Caricato M, Li X, Hratchian H P, Izmaylov A F, Bloino J, Zheng G, Sonnenberg J L, Hada M, Ehara M, Toyota K, Fukuda R, Hasegawa J, Ishida M, Nakajima T, Honda Y, Kitao O, Nakai H, Vreven T, Montgomery J A, Jr, Peralta J E, Ogliaro F, Bearpark M, Heyd J J, Brothers E, Kudin K N, Staroverov V N, Kobayashi R, Normand J, Raghavachari K, Rendell A, Burant J C, IyengaSr S S, Tomasi J, Cossi M, Rega N, Millam M J, Klene M, Knox J E, Cross J B, Bakken V, Adamo C, Jaramillo J, Gomperts R, Stratmann R E, Yazyev O, Austin A J, Cammi R, Pomeli C, Ochterski J W, Martin R L, Morokuma K, Zakrzewski C G, Voth G A, Salvador P, Dannenberg J J, Dapprich S, Daniels A D, Farkas O, Foresman J B, Ortiz J V, Cioslowski J

& Fox D J, Gaussian 09, Revision A.02, Gaussian, Inc, Wallingford CT, 2016.
23 Ditchfield R, *Mol Phys,* 27 (1974) 789.
24 Wolinski K, Hinton J F & Pulay P, *J Am Chem Soc*, 112 (1990) 8251.
25 Murray J S & Politzer P, *WIREs Comput Mol Sci*, 1 (2011) 153.
26 Bavara S, *Asian J Chem,* 22 (2010) 5237.
27 Koopmans T A, *Physica*, 1 (1934) 104.
28 Frisch M J, Nielsm A B & Holder A J, *Gaussview User Manual*, Gaussian Inc, Pittsburgh, 2008.
29 Silverstein R M & Webster F X, Spectroscopic Identification of Organic Compounds, (Wiley, New York), 6th Edn, 2005.
30 Scalmani G & Frisch M J, *Chem Phys,* **132** (2010) **114110.**
31 Krygowski M T, Cyran M K, Czarnocki Z, Hafelinger G & Katritzky A R, *Tetrahedron*, 56 (2000) 1783.
32 Schleyer P R, Maerker C, Dransfeld A, Jiao H & Hommes N J R E, *J Am Chem Soc*, 118 (1996) 6317.
33 Bayar C C & Turker L, *Polycycl Aromat Compd,* 40 (2020) 1266.
34 Ebrahimi A, Karimi P, Akher F B, Behazin R & Mostafavi N, *Mol Phys*, 112 (2014) 1047.
35 Pausescu I, Medeleanu M, Stefanescu M, Peter F & Pop R, *Heteroatom Chem*, 26 (2015) 206.
36 Fleming I, Frontier Orbitals and Organic Chemical Reactions (Wiley, London), 1976.
37 Rocha M, Santo A D, Arias J M, Gil D M & Altabef A B, *Spectrochim Acta A*, 136 (2015) 635.
38 Singh V D, Uppal A, Kamni, Khajuria Y, Srinivasan R, Narayan B, Sarojini B K, Anthale S & Kant R, *Indian J Chem*, 59B (2020) 1043.
39 Özer Z, Kılıç T, Çarıkçı S & Azizoglu A, *Russ J Phys Chem A*, 93(2019) 2703.
40 Prasad L G & Raman R G, *Indian J Pure Appl Phys*, 59 (2021) 138.
41 Pearson R G, Chemical Hardness, (Wiley, New York), 1997.
42 Luque F J, Lopez J M & Orozco M, *Theor Chem Acc*, 103 (2000) 343.
43 Vijay D, Priya Y S, Satyavani M, K, Rajasekhar B N & Veeraiah A, *Spectrochim Acta A*, 229 (2020) 117930.
44 Rani V, Tyagi A & Kumar A, *Indian J Pure Appl Phys*, 59 (2021) 48.
45 Reed A E, Curtiss L A & Weinhold F, *Chem Rev*, 88 (1988) 899.
46 Sen I, Yıldız C B, Kara H & Azizoglu A, *Phosphorus Sulfur Silicon Relat Elem,* 188 (2013) 1621.